Composites Part B 167 (2019) 51–62

Contents lists available at ScienceDirect

Composites Part B

journal homepage: www.elsevier.com/locate/compositesb

Automated generation of carbon nanotube morphology in cement composite via data-driven approaches

Hyeong Min Park[a,b,1], S.M. Park[c,1], Seung-Mok Lee[d], In-Jin Shon[b], Haemin Jeon[e,**], B.J. Yang[a,*]

[a] Institute of Advanced Composite Materials, Korea Institute of Science and Technology, 92 Chudong-ro, Bongdong-eup, Wanju-gun, Jeollabuk-do, 55324, Republic of Korea
[b] Division of Advanced Materials Engineering, Chonbuk National University, 567 Baekje-daero, Deokjin-gu, Jeonbuk, 54896, Republic of Korea
[c] Department of Civil and Environmental Engineering, Korea Advanced Institute of Science and Technology, 291 Daehak-ro, Yuseong-gu, Daejeon, 34141, Republic of Korea
[d] Department of Mechanical and Automotive Engineering, Keimyung University, 1095 Dalgubeol-daero, Dalseo-gu, Daegu, 42601, Republic of Korea
[e] Department of Civil and Environmental Engineering, Hanbat National University, 125 Dongseodae-ro, Yuseong-gu, Daejeon, 34158, Republic of Korea

ARTICLE INFO

Keywords:
Micromechanics
Particle swarm optimization
Data driven model
Electrical resistivity
Cement composite
Hierarchical conductivity structure

ABSTRACT

Electrified cement composite has attracted considerable attention in major scientific and engineering fields due to its excellent functional characteristics. With increasing interest in this functional material, the need for an advanced theoretical approach has also increased significantly. In the present study, a data-driven model based on hierarchical micromechanics and particle swarm optimization is proposed to estimate the morphological characteristic of conductive nanofiller of cement composites. Experimental data needed for the simulation are acquired by fabricating cement specimens with various contents of multi-walled carbon nanotube (MWCNT), carbon fiber, and water-to-cement ratios, and measuring their electrical resistivity, porosity, and aspect ratio by relevant experimental and computational techniques. Based on the proposed framework, a series of numerical simulations including the experimental comparisons of the electrified cement composite are carried out to clarify the potential of the present model. The number of model parameters is reduced to the curviness of MWCNT, which is the most influential model parameter, and the process of collecting and simplifying the pattern is included.

1. Introduction

The paradigm of material modeling has been characterized by the formulation of physical and mathematical laws; however, the theories of material science became increasingly complex over time, diminishing its effectiveness [1]. For construction materials, the undesirable phenomenon has recently accelerated, whereby the composition of materials has become more complicated due to the incorporation of various admixtures [2,3]. The reason for adding admixtures to cement material is to enhance functionality in construction. The types of cement based construction materials are: (1) those most exposed to the atmosphere, (2) those frequently contacted with humans, (3) those that are the least expensive, and (4) those that are the most consumed [4]. The development of unique functionality in construction materials is therefore expected to facilitate considerable innovation for the future.

Among the various studies on the development of such functionality in construction materials, studies are being actively carried out to improve the electrical conductivity of construction materials. Recent studies have shown that incorporating conductive fillers such as carbon nanotubes (CNTs) and carbon fibers (CFs) increases the electrical properties of cement to a semiconductor level. It is expected that construction materials with high electrical conductivity have a high impact on science and industry in the future since they have various applications such as for self-deicing road systems [5,6], electromagnetic shielding wall [3,7], and in the damage sensing, energy harvesting [8,9], and monitoring of infrastructures [10].

While the experimental works for investigating construction materials are a much-attempted research endeavor (Table 1), rigorous theoretical simulation of cementitious composites is rarely reported. Many phenomena observed in cement-based composites remain unexplained by existing classical models. A number of attempts were made by employing the first principles method [11,12] and molecular dynamics

* Corresponding author.
** Corresponding author.
E-mail addresses: hjeon@hanbat.ac.kr (H. Jeon), bj.yang@kist.re.kr (B.J. Yang).
[1] Theses authors contributed equally to this work.

https://doi.org/10.1016/j.compositesb.2018.12.011
Received 20 July 2018; Received in revised form 19 November 2018; Accepted 3 December 2018
Available online 07 December 2018
1359-8368/ © 2018 Elsevier Ltd. All rights reserved.

Table 1
Literature studied for improving the electrical characteristic of cement paste.

CNT dispersion method in cement	Effect	Ref.
Sonication	It is the earliest dispersion method of CNT in the cement binder. An improved electrical conductivity of cement composites can be achieved; however, the morphology of CNT is broken and deformed into a flake-like shape during the process.	[17]
Addition of silica fume	The silica fume in the form of nanoparticles serves as a bearing between the CNTs, and thus it mechanically induces dispersion of fillers.	[17,18]
W/C control	The extremely reducing W/C reduces the amount of porosity in cement binder during the hydration process, and increases the electrical conductivity of the specimen.	[18]
Addition of superplasticizer	The addition of a superplasticizer to the above combination induces chemical modification on the CNT surface. It overcomes the viscosity problems and leads the improved workability of the cement specimens.	[16]
Addition of CF	By adding CF, the durability of the specimen can be improved by connecting the electrical pathway composed with CNTs as well as bridging effect.	[19]

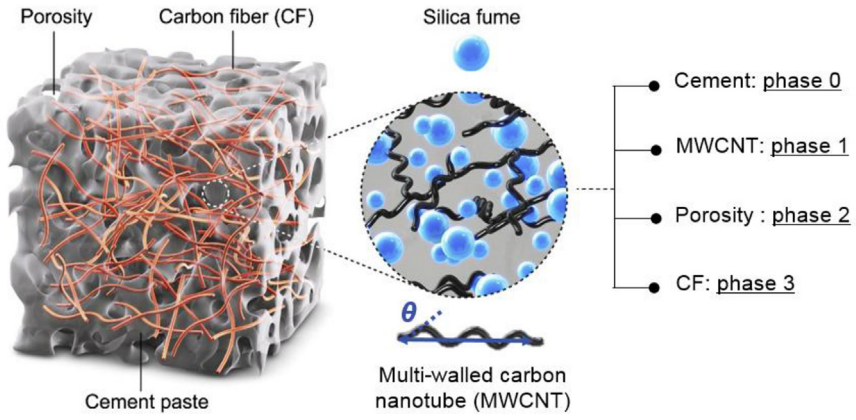

(a)

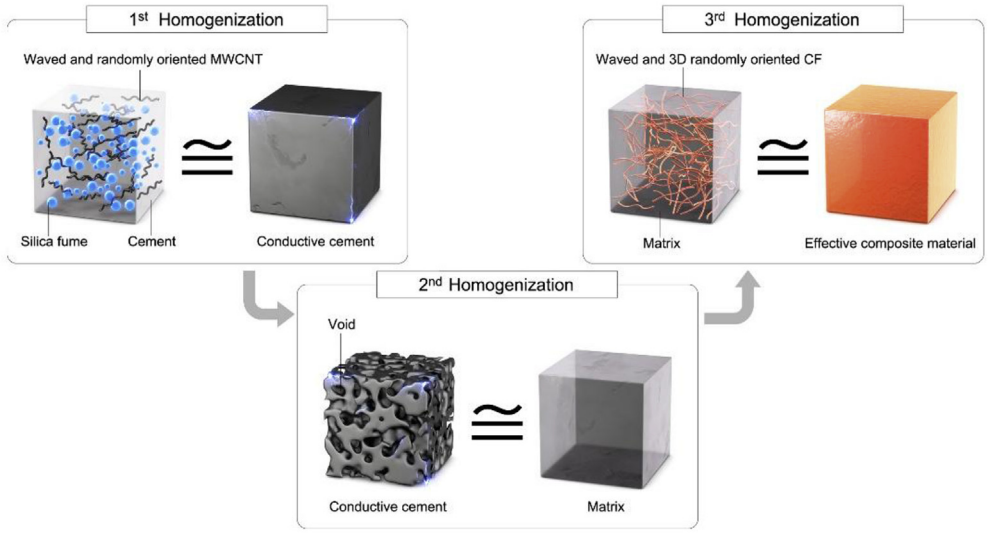

(b)

Fig. 1. (a) Overview of the hierarchical conductive cement composites and (b) three-level homogenization process based on the micromechanical model.

(MD) simulations [13,14], while the calculation results present significant deviation among theories and much computational resources are required. In addition, the simulation tool used to quantitatively predict the unique behavior of electrified cement materials is insufficient. Herein, we propose a reliable theoretical framework that comprises experimental data, a computational algorithm (particle swarm optimization, PSO), and micromechanics. Through the proposed model, it is expected that the functions and mechanisms of the cement-based smart composites are analyzed in depth [15]. To the best of our knowledge, this is the first attempt to combine the data-driven

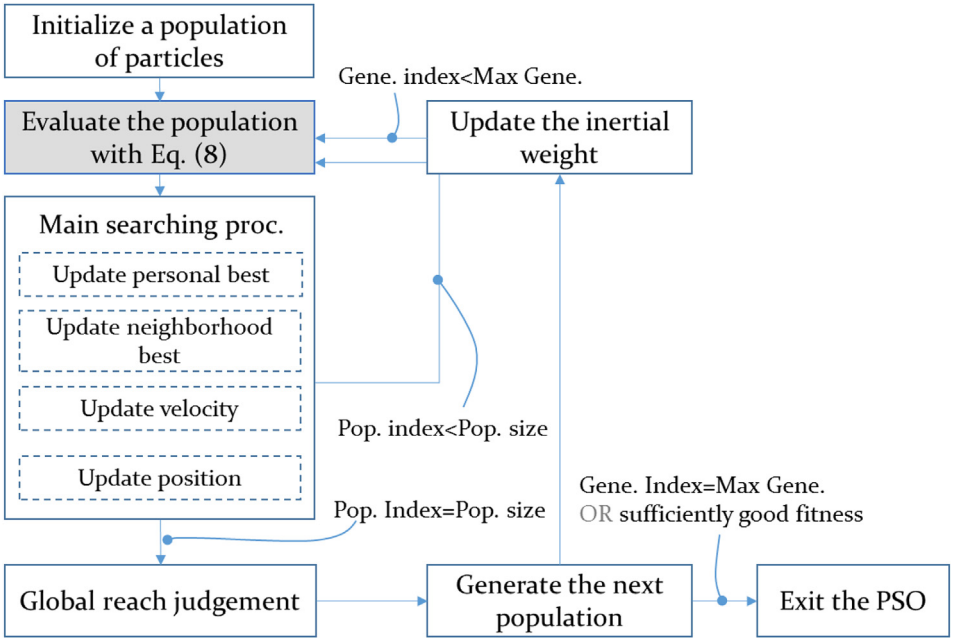

Fig. 2. Computational flow chart for the combination of micromechanical model and PSO algorithm.

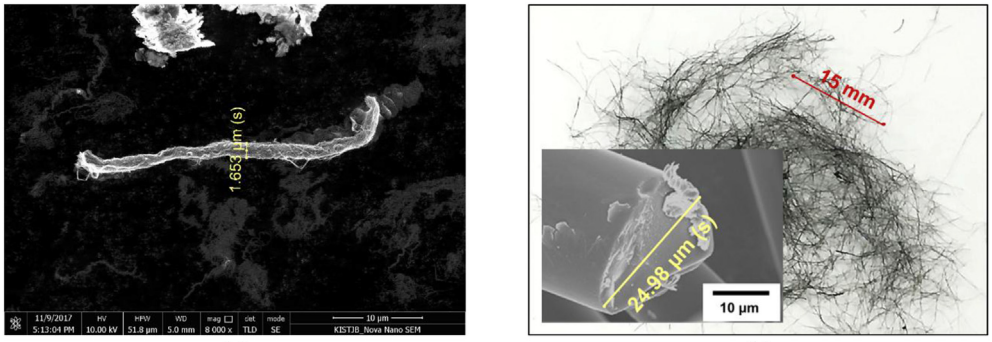

Fig. 3. Length and diameter of utilized (a) MWCNTs and (b) CF.

technique with evolutionary computation and analytical model for highly electrified cement composites.

In the present study, a simulation method combining the PSO algorithm and micromechanics is newly proposed to overcome the difficulties of accurately understanding the electrified cementitious materials. The selected target material for the simulation is cement composite containing multi-walled carbon nanotubes (MWCNTs) and CF, which is reported to be economically competitive and have excellent durability [16]. To accurately model the change occurring in the hierarchical conductivity structures within cement composites at a nano- and micro-scale, micromechanics-based homogenizations are performed in three stages with respect to the scale. In addition, to model the characteristics of cement composites more realistically, the micromechanical model is designed to consider the porosity in the specimen and the waviness of the MWCNTs. The model constants required for the simulation are obtained by analyzing experimental results using the PSO algorithm, and the pattern of parameters according to the change of material compositions is estimated.

To generate the experimental data needed for the simulation, conductive cement composite specimens with various contents of MWCNT, CF, and water-to-cement ratios (W/C) are fabricated. In the experimental study, silica fume and surfactant are also included to provide fine dispersion of fillers with reference to the existing literature [17,18]. The electrical resistivity of the fabricated specimens is measured using the two-probe method. In addition, image processing technique-based in-house software is built to measure the exact length of the wavy MWCNT, which is a critical input parameter of the present proposed model. Since no clear standard is available to measure the porosity of cement composite, the porosity is analyzed using thermographic and micro-computed tomography (CT) analyses.

2. Theories

2.1. Micromechanics-based model

It is important to note that the present study deals with a multi-phase complex material. Let us consider that the multi-phase material consists of cement (phase 0), MWCNT (phase 1), porosity (phase 2), and CF (phase 3), and that phases 1–3 are randomly and uniformly dispersed in phase 0 (Fig. 1(a)). For simplicity, it is assumed that the electrical characteristics of cement and silica fume are the same based on the previous studies [19]. To theoretically simulate the *cementitious* complex material, we carried out a micromechanics-based *multiscale* homogenization process consisting of three steps [20–25]. The purpose of this is to treat the complex material, which contains more than two phases, as one plain phase by applying mathematical techniques [26]. The following three-step homogenization process was carried out here, considering the length scale of each material. The corresponding

Table 2
Mix proportion of electrified cement paste to be used for the PSO algorithm (wt. %).

Specimen	Cement	CNT	CF	Silica fume	Superplasticizer	Water
C0F0W1	100	0	0	20	1.6	30
C0F0W2						35
C0F0W3						40
C0F0W4						45
C0F1W1			0.1			30
C0F1W2						35
C0F1W3						40
C0F1W4						45
C0F5W1			0.5			30
C0F5W2						35
C0F5W3						40
C0F5W4						45
C1F0W1	100	0.1	0	20	1.6	30
C1F0W2						35
C1F0W3						40
C1F0W4						45
C1F1W1			0.1			30
C1F1W2						35
C1F1W3						40
C1F1W4						45
C1F5W1			0.5			30
C1F5W2						35
C1F5W3						40
C1F5W4						45
C2F0W1	100	0.5	0	20	1.6	30
C2F0W2						35
C2F0W3						40
C2F0W4						45
C2F1W1			0.1			30
C2F1W2						35
C2F1W3						40
C2F1W4						45
C2F5W1			0.5			30
C2F5W2						35
C2F5W3						40
C2F5W4						45
C3F0W1	100	1.0	0	20	1.6	30
C3F0W2						35
C3F0W3						40
C3F0W4						45
C3F1W1			0.1			30
C3F1W2						35
C3F1W3						40
C3F1W4						45
C3F5W1			0.5			30
C3F5W2						35
C3F5W3						40
C3F5W4						45
C4F0W1	100	2.0	0	20	1.6	30
C4F0W2						35
C4F0W3						40
C4F0W4						45
C4F1W1			0.1			30
C4F1W2						35
C4F1W3						40
C4F1W4						45
C4F5W1			0.5			30
C4F5W2						35
C4F5W3						40
C4F5W4						45

contents are described in Fig. 1(b).

The first homogenization step involves materials at a nanoscale, including cement, silica fume, and MWCNT. The effective medium theory (EMT) model [27] is considered in this step. The EMT model has been proven in many studies to be adequate for predicting the electrical conductivity of composite materials [27,28]. The homogenization of cement binder (phase 0) and MWCNT (phase 1) is then performed using the EMT equation as follows [29]:

$$(1-\phi_1)[(L_0-L_{cc})^{-1}+L_0^{-1}/3]^{-1}+\phi_1[\{L_1-L_{cc}\}^{-1}+\mathbf{S}_1L_{cc}^{-I}]^{-1}=0 \quad (1)$$

where L_r and ϕ_r refer to the electrical conductivity tensor and volume fraction of r-phase, respectively, and the subscripts 0, 1, and cc denote the material phases of cement, MWCNT, and conductivity cement, respectively. From a theoretical viewpoint, the materials are generally assumed to be in an ideal state, although this is often not the case in reality [26]. For example, it is theoretically assumed that the MWCNT filler is fully extended within the matrix; however, such a case is impossible in reality, due to the lengthy aspect ratio of CNTs and the high viscosity of matrix [30,31]. Therefore, in this paper, the waviness characteristics of MWCNT is considered as model constants and are defined θ (Fig. 1(a)). $\mathbf{S}_r$ signifies the aspect ratio dependent depolarization tensor, which can be expressed as follows [32].

$$(S_{11})_1=(S_{22})_1=\frac{\alpha_1^w}{2\{(\alpha_1^w)^2-\alpha_1^w\}^{3/2}}[\alpha_1^w\{(\alpha_1^w)^2-1\}^{1/2}-\cosh^{-1}\alpha_1^w]$$
$$(S_{33})_1=1-2(S_{11})_1 \quad (2)$$

where the superscript w refers to the waviness effect that occurs in the filler; α denotes the aspect ratio (l_r/d_r); l_r and d_r are the length and diameter of r-phase, respectively. The aspect ratio of MWCNT considering waviness effect can be calculated as follows

$$\alpha_1^w=\frac{4\pi l_1}{\tan(\theta)\{2l_1+d_1l(\theta)\}} \quad (3)$$

with

$$l(\theta)=\int_0^{\frac{2\pi}{\tan\theta}}\sqrt{1+[\tan\theta\{-\sin(x\tan\theta)\}]^2}\,dx \quad (4)$$

In Eq. (5), θ denotes the degree of waviness when the spheroidal filler is assumed to be waved to a sinusoidal curve. A more detailed description of the bending of the filler with respect to the sine curve can be found in Ref. [19].

The second homogenization step is performed on the conductive matrix and pores. The porosity (ϕ_2) significantly affects the overall performance of the hydrated cement, and must be considered to predict the precise material behavior [33]. The pores are distributed over nano and micro scales, and thus they are preferably placed in the second homogenization, which is between the nano and micro levels. Considering the computational cost, the Mori-Tanaka (MT) model is utilized at the second homogenization. The applicability of the EMT model for simulating the electrical properties of materials has been verified in numerous studies. However, the disadvantage of the EMT model is that it must be solved numerically because the equation is not explicitly expressed. It inevitably requires a considerably high level of computation time. The MT model, on the other hand, consists of a simple form in which the result is computed directly for given input values. Thus, the MT model for calculating the conductive cement matrix containing porosity is expressed as follows [29].

$$L_m=L_{cc}+\phi_2[I-\phi_2\{(L_2-L_{cc})^{-1}+L_{cc}^{-1}/3\}^{-1}L_{cc}^{-1}/3]^{-1}\{(L_2-L_{cc})^{-1}+L_{cc}^{-1}/3\}^{-1} \quad (5)$$

where I and the subscript m denote the identical tensor and the matrix, respectively. L_{cc} is the result of Eq. (1) calculated by the first homogenization, and the definitions of the remaining constants are described above. Herein, the key constant of ϕ_2 is experimentally measured via the thermographic image and the micro-CT methods, which are described in the Experimental section.

Finally, the third homogenization step involving CFs (the largest constituent material) and the matrix is carried out. In the third homogenization step, the EMT model is applied similarly to the first homogenization. Most theoretical expressions are thus similar; however, the waviness effect of CFs are not considered based on the scanning electron microscopy (SEM) images analysis. Further details of the SEM results are given in the Results and discussion section.

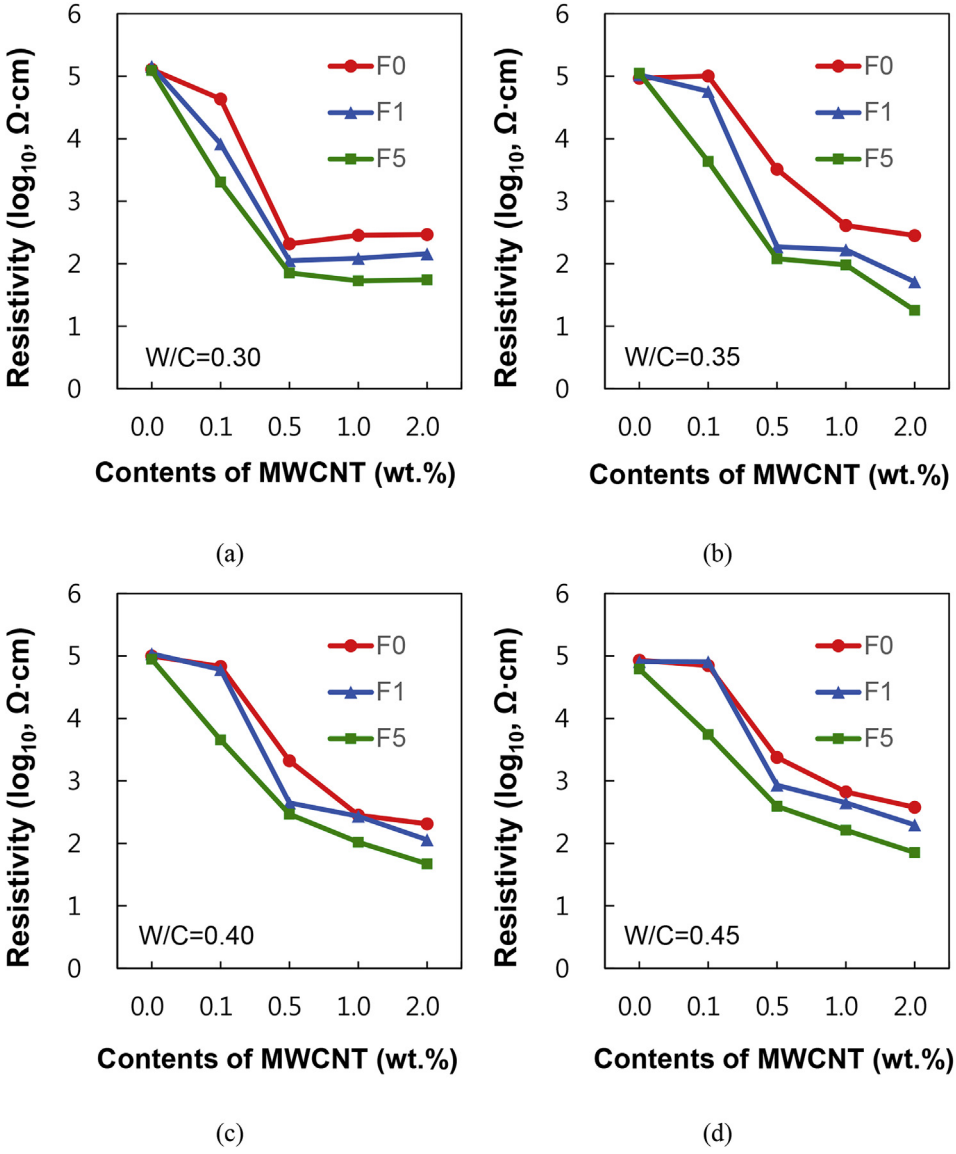

Fig. 4. Experimentally measured electrical resistivities of the MWCNT/CF-embedded cement composites with various W/C values: (a) 0.30, (b) 0.35, (c) 0.40, and (d) 0.45.

$$(1-\phi_3)[(L_m-L_e)^{-1}+L_m^{-1}/3]^{-1}+\phi_3[\{L_3-L_m\}^{-1}+\mathbf{S}_3L_e^{-1}]^{-1}=0 \quad (6)$$

where the subscript e denotes the effective value of the entire complex material, and $\mathbf{S}_3$ is

$$(S_{11})_3=(S_{22})_3=\frac{\alpha_3}{2\{(\alpha_3^w)^2-\alpha_3^w\}^{3/2}}[\alpha_3\{(\alpha_3)^2-1\}^{1/2}-\cosh^{-1}\alpha_3]$$
$$(S_{33})_3=1-2(S_{11})_3 \quad (7)$$

where α_3, l_3, and d_3 denote the aspect ratio, length, and diameter of CF, respectively.

2.2. Application of PSO algorithm

In this paper, the particle swarm optimization (PSO) algorithm which provides quick results even with multiple objectives and constraints, is used to find the hyperparameters of the proposed constitutive equation [34–37]. The PSO algorithm is a population-based metaheuristic optimization method proposed by Kennedy and Eberhart [36].

Similar to other evolutionary algorithms, the PSO algorithm is initialized with a population of random solutions in given boundaries and the solutions (also called particles) move toward better search areas via cooperation and competition among the population [34]. However, it also assigns a randomized velocity to accelerate each particle toward its personal and neighborhood best solutions. In other words, a number of neighbors are assigned to each particle and the particle is updated considering its experiences and neighbors by repeating iteration [35]. The position and velocity are updated by the following equations:

$$x_{id}=x_{id}+v_{id}$$
$$v_{id}=w\cdot v_{id}+c_1\cdot r_1\cdot(p_{id}-x_{id})+c_2\cdot r_2\cdot(p_{gd}-x_{id}) \quad (8)$$

where x_{id} and v_{id} denote the position and velocity of the i-th particle in d-dimension, c_1 and c_2 are the self and social acceleration coefficients, and p_{id} and p_{gd} are the personal and neighborhood bests, respectively. w is the inertial weight, and r_1 and r_2 are random number in the domain of [0,1]. The PSO algorithm is combined with the micromechanical theory for the simultaneous analysis of various specimens with different W/C, MWCNT, and CF contents. By minimizing the difference between the simulation and experimental results, the parameter set (x_{id}) in Eq. (12) is adjusted. The simulation flow chart for the combination of the micromechanical model and PSO algorithm is shown in detail in Fig. 2.

Considering the computational implementation, the

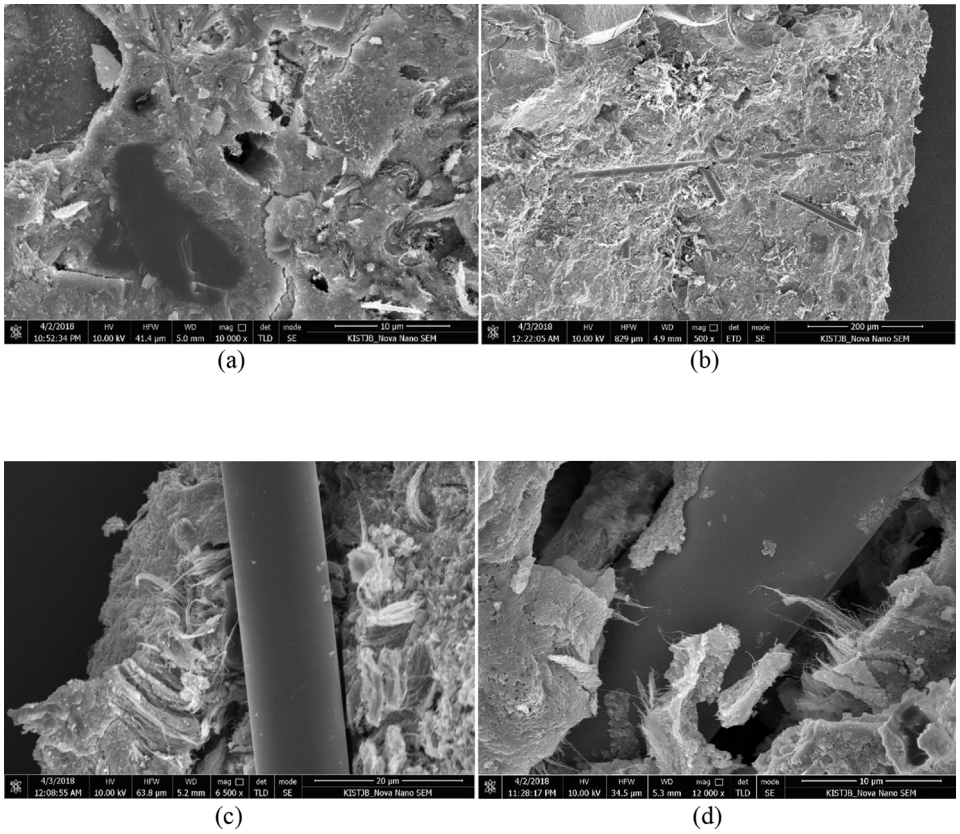

Fig. 5. SEM images of the internal structure in cement composite: (a) porosity distributed in various sizes in cement matrix and (b) straight CFs embedded in the cement matrix, (c) MWCNTs that are heavily curved relative to CF, and (d) hierarchical conductivity structure consisting of MWCNT and CF.

micromechanical equations are explicitly derived and arranged according to the following calculation process:

1. Define input parameters
   - Material characteristics:
     - ✓ Electrical conductivity of cement, MWCNT, porosity, and CF: $L_{0,\ 1,\ 2,\ 3}$
     - ✓ Volume fraction of MWCNT and CF: $\phi_{1,3}$
     - ✓ Diameter of MWCNTs: d_1
     - ✓ Length and diameter of CF: l_3 and d_3
     - ✓ Water/cement ratio: W/C
   - Model constants:
     - ✓ Waviness degree of MWCNT: θ
     - ✓ Length of MWCNTs: l_1
     - ✓ Volume fraction of porosity: ϕ_2
2. Calculate simulation constants
   - Depolarization tensor: $S(_{11,\ 22,\ 33})_{1,3}$ in Eqs. (2) and (7)
   - Aspect ratio of MWCNT with waviness effect: $(\alpha_1)^w$ in Eq. (3)
3. First homogenization
   - Assuming that the electrical conductivity of MWCNT is isotropic, Eq. (1) can be explicitly rephrased as follows:

$$\frac{3(1-\phi_1)(\sigma_0-\sigma_{cc})}{\sigma_0+2\sigma_{cc}}+\frac{\phi_1}{3}\left[\frac{2\{\sigma_1-\sigma_{cc}\}}{\sigma_{cc}+\{\sigma_1-\sigma_{cc}\}+(S_{11})_1}+\frac{\sigma_1-\sigma_{cc}}{\sigma_{cc}+\{\sigma_1-\sigma_{cc}\}+(S_{33})_1}\right]=0 \tag{9}$$

where σ_r denotes the isotropic electrical conductivity of r-phase.

4. Second homogenization
   - Assuming that the shape of the porosity is spherical, Eq. (5) can be explicitly rephrased as follows:

$$\sigma_m=\sigma_{cc}\left[\frac{3(2\sigma_{cc}+\sigma_2)}{\sigma_{cc}(\phi_2+2)-\sigma_2(\phi_2-1)}-2\right] \tag{10}$$

5. Third homogenization
   - Assuming that the electrical conductivity of CF is isotropic, Eq. (6) can be explicitly rephrased as follows:

$$\frac{3(1-\phi_3)(\sigma_m-\sigma_e)}{\sigma_m+2\sigma_e}+\frac{\phi_3}{3}\left[\frac{2\{\sigma_3-\sigma_m\}}{\sigma_m+\{\sigma_3-\sigma_m\}+(S_{11})_3}+\frac{\sigma_3-\sigma_m}{\sigma_m+\{\sigma_3-\sigma_m\}+(S_{33})_3}\right]=0 \tag{11}$$

6. Population updates
   - Evaluate the accuracy of micromechanical simulation with experimental data.
   - Update the personal best, neighborhood best, velocity, and position until the population index reach the previously set population size.
   - Generate the next population and update the inertial weight until the maximum generation number is reached or the fitness is satisfied.
   - The inertial weight range is set to [0.1, 1.1]; c_1 and c_2 are set to 1.49, and neighborhood size is 12, with a swarm size of 50. The swarm size is determined by considering the accuracy and computation time, and detailed calculations are represented in Fig. 8(b).

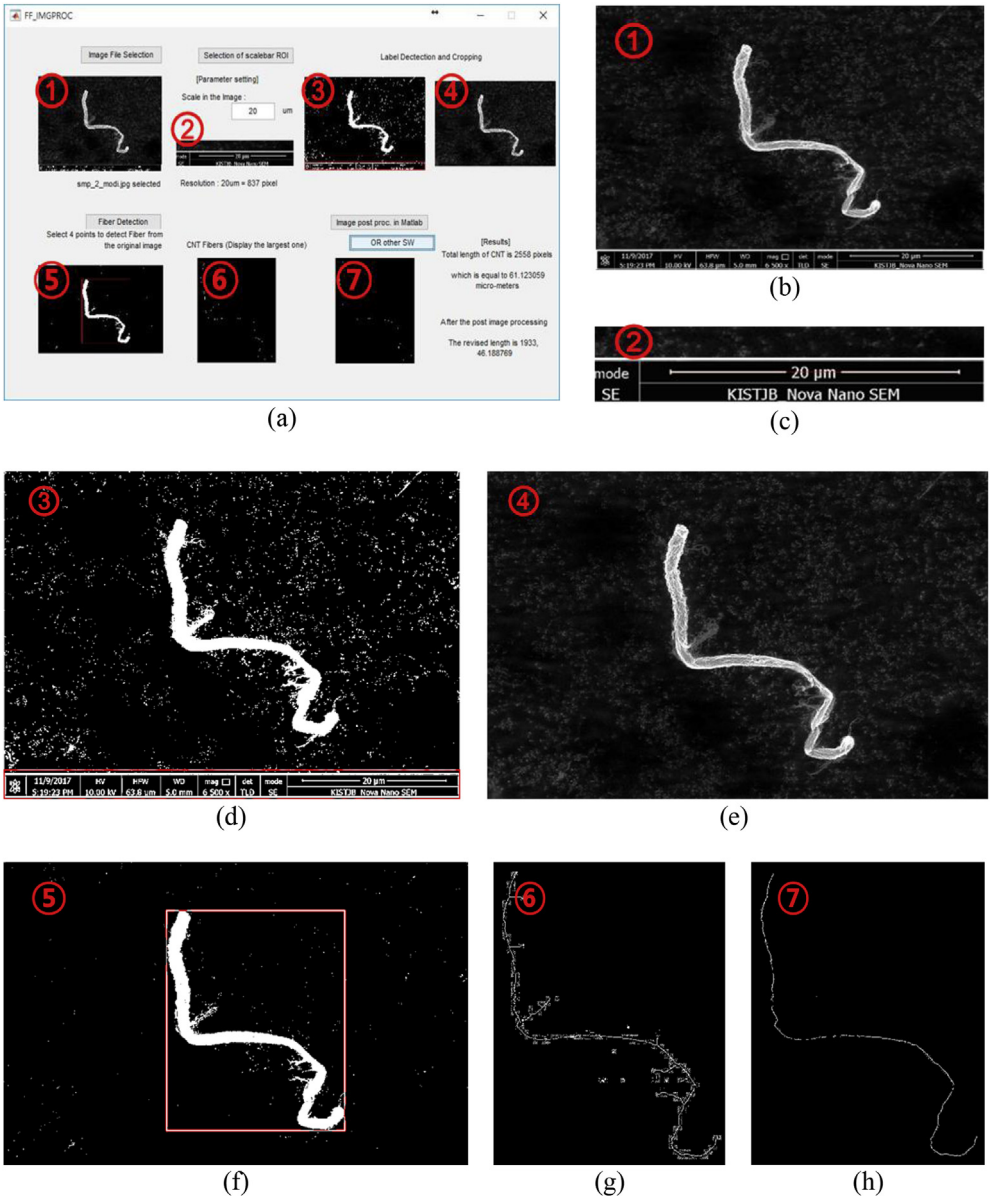

Fig. 6. Process of evaluating the effective length of wavy MWCNT: (a) Overall appearance of developed in-house software, (b) original SEM image of MWCNT, (c) scale bar of the selected image, (d) initial result of black and white conversion, (e) remaining image after performing the previous steps, (f) second image processing result and automatically selected analysis area, (g) center line of image represented as a vector, and (h) all vectors eliminated except the largest value.

3. Experiments

3.1. Materials and fabrication

The main obstacles hindering the commercialization of highly electrified cement composite are as follows: (1) it has a relatively high production cost compared with conventional construction materials, and (2) while the mix design is optimized to reach high electrical conductivity, other fresh and hardened state properties may not necessarily be as satisfactory as those of another construction material. In the present study, the MWCNT with a purity of 98.5% (Jeno Tube 8 ©) by Jeio Co. Ltd.) and pitch based CF (GS Caltex Co.) were used together in order to overcome the excessive use of MWCNT and the performance degradation due to the increase of W/C. It is noted that the purity of MWCNT used in the present study is much lower than that of other commercially available nanotubes; it was selected for its significantly low cost (100$/kg), rendering it more commercially viable for construction applications. The length and diameter of MWCNT and CF used in this study are shown in Fig. 3(a) and (b).

Dispersion of CNT and CF fillers throughout the cement matrix is mandatory for developing high conductivity, and can be achieved using silica fume and superplasticizer [30,38]. Type I ordinary Portland cement and silica fume (EMS-970 manufactured by Elkem Inc.) were used as a binder material to disperse CNT and CF fillers uniformly, and a polycarboxylic-acid-based superplasticizer (GLENIUM 8008 by BASF Pozzolith Ltd.) was used to decrease the Van der Waals forces on the MWCNT and improves workability. Table 2 shows the mix proportion of specimens used in the present study. Specimens with various contents of conductive fillers were prepared to investigate the effect of conductive fillers on the electrical characteristics. For all specimens, the silica fume and the superplasticizer were used at 20.0 and 1.6%, respectively, by the mass of cement. The MWCNT contents were 0.0, 0.1, 0.5, 1.0, and 2.0 wt% and the CF contents were 0.0, 0.1 and 0.5 wt%.

The fabrication processes of the specimen are as follows: dry materials (cement, silica fume, MWCNT and CF) were blended for 1 min using a mortar mixer (Heungjin, HJ-1150). A mixture of water and

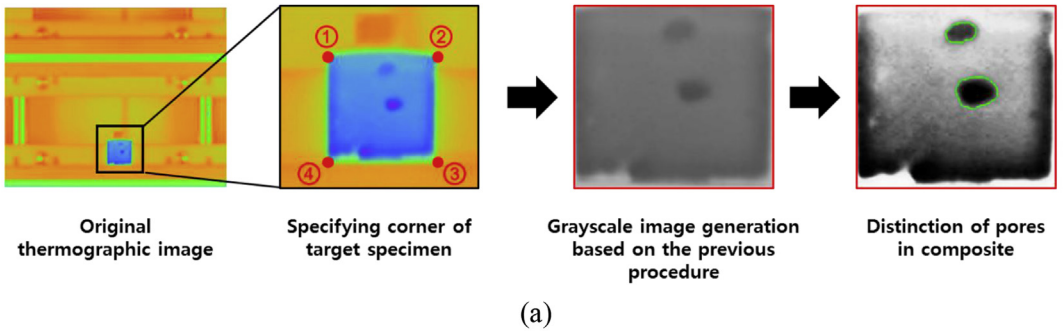

(a)

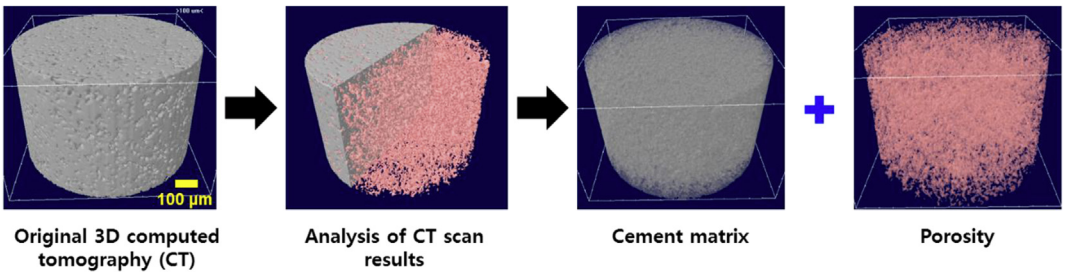

(b)

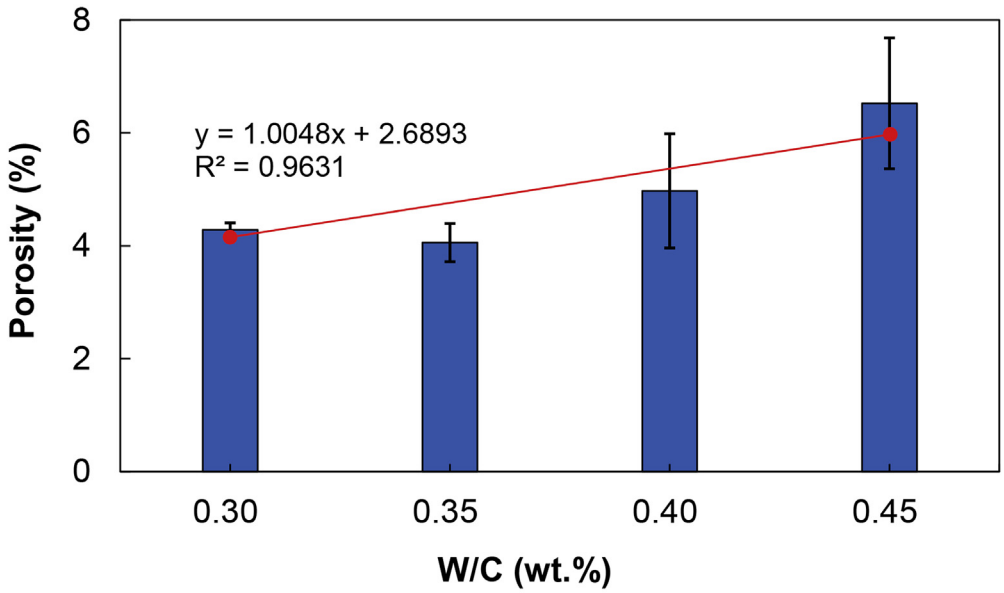

(c)

Fig. 7. Process of porosity measurement in cement composite via (a) thermographic image, (b) micro CT scan analyses, and (c) the calculated porosity values with various W/Cs.

superplasticizer was added to the dry materials, and mixed for another 5 min. The fresh mortar was poured into a 25 mm^3 cubic mold. For all specimens, two copper electrodes were inserted into the fresh mortar specimens at 10 mm intervals to measure the resistance of the specimens. The height and width of the copper electrodes were 30 mm and 10 mm, respectively. The mold was then sealed and cured to minimize evaporation of water.

3.2. Characteristics

The electrical resistance was measured by a two-probe method using a multimeter (FLUKE, True-rms Multimeter), and the resistance was converted into the resistivity by applying the following equation

$$\rho = R \cdot \frac{A}{L} \tag{12}$$

where ρ and R indicate the resistivity ($\Omega \cdot cm$) and the measured electrical resistance (Ω), respectively, and L and A indicate the distance between the copper electrodes and the cross-section area of the electrode inserted in the cement block, respectively.

Scanning electron microscopy (SEM) images were captured using NOVA Nano SEM 450 to analyze the surface morphology and microstructure of the specimens. Fractured samples were collected from the corresponding specimens, and were coated with Pt in a low vacuum prior to the SEM analysis.

In addition, the internal porosities of the fabricated specimens were quantitatively measured using a nondestructive inspection technique

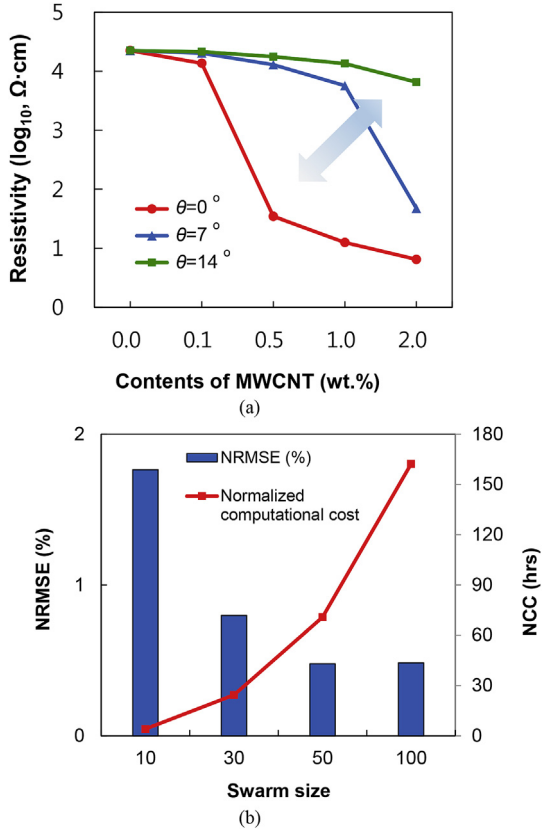

Fig. 8. (a) Predicted electrical resistivity of cement composites with various model parameters: interfacial resistivity of MWCNT and (b) the effect of swarm size on the normalized root mean square error (NRMSE) and normalized computational cost (NCC).

based on the use of a thermal imaging camera and micro CT analysis. The thermal image was obtained by placing the specimen 1 m from the thermal imaging camera (FLIR, x6540sc) and exposing it to the heat from two halogen lamps 5 times for 5 s to measure the changed heat. Cylindrical specimens with a diameter of 5 mm and a length of 7 mm, respectively, and with different W/Cs (0.30, 0.35, 0.40, and 0.45) were separately prepared for micro-CT analysis. The micro-CT analysis was conducted on a SkyScan 1172 (Bruker) using an Al + Cu filter and small camera pixels (4 K × 2 K) at 1.7 μm resolution, with a source voltage of 100 kV, a source current of 100 μA, and specimen rotation angles of 360°.

4. Results and discussion

4.1. Electrical resistivity

Fig. 4 presents the electrical resistivity of the specimens with respect to the MWCNT and CF contents, and W/C. It was found that the electrical resistivity decreases with increasing content of MWCNT content, regardless of W/C. In particular, the resistivity decreased more effectively when the contents of MWCNT and CF were increased. According to previously reported studies [30], the combination of MWCNT and CF induces a synergistic effect known as the bridging effect. Hence, it is assumed that the increase in the content of MWCNT and CF leads to further improvement of the connectivity of the conductive network within the binder matrix.

SEM images of the cement composite containing MWCNT and CF are shown in Fig. 5. It can be seen in Fig. 5(a) and (b) that the pores with various sizes are randomly distributed along the binder matrix, and the CFs are mostly distributed in a fully extended state. Fig. 5(c) and (d) show that the MWCNTs that are heavily curved relative to CF and that MWCNT and CF are intertwined with each other. It notes that the pores with various sizes and the waved MWCNTs in the cementitious matrix play a role in reducing conductive connectivity, and have a negative effect on the overall electrical characteristics. However, the conductive bridge between CF and MWCNT serves to inhibit this phenomenon, as shown in Fig. 5(d).

4.2. Evaluation of simulation input data

Determining of the input values for the theoretical analysis is an essential factor affecting the overall reliability of the simulation study. Particularly, the length and diameter of conductive fillers, which directly affect the conductive path, are the most critically evaluated factors. The length of the CF and the diameters of the CF and MWCNT are relatively easy to measure with an optical microscope. However, accurately defining a representative length of MWCNT is difficult, which is randomly distributed and variously curved at the nanoscale. Hence, in this study, SEM images of various MWCNTs are randomly selected and the exact length of the curved nanotubes on the image is calculated by applying the image processing technique.

Simple in-house software is built to measure the exact length of the waved MWCNT, and the overall user interface is shown in Fig. 6(a). First, the original SEM image of MWCNT is selected for analysis (Fig. 6(b)), and the real size of the selected image is defined by referring to the scale bar in the photograph (Fig. 6(c)). Then, the selected photo is divided into the black and white converted image (Fig. 6(d)) and the original image (Fig. 6(e)). The processed image shown in Fig. 6(d) is again subjected to image processing with a higher criterion (Fig. 6(f)), and the object to be analyzed is automatically captured, as shown in the red boxes. The results of the previous analysis steps are shown in Fig. 6(g). By deleting the remaining parts except for the largest vector in Fig. 6(g), the length of MWCNT to be obtained can be calculated (Fig. 6(h)).

The porosity measurement for the cement composite specimens is carried out via thermographic and micro-CT analyses, as shown in Fig. 7. While water inevitably causes pores to form in all hydrated cement, no standardized protocol has been available for accurately measuring the porosity of hydrated cement. In this study, the macro-sized porosities are quantitatively measured using a thermographic image (Fig. 7(a)). The size of the photographed thermal image is artificially selected to be the size necessary for analysis, and the porosities are then measured through image analysis. Fig. 7(b) schematically shows the process of estimating the volume fraction of micro-sized porosity based on the 3D scan data taken from the micro-CT. The original 3D CT data can be divided into solid and air due to the difference in the electromagnetic wave transmittance, and the quantitative value of porosity is precisely measured. Considering the limits of the measurable scale of the above two methods, the volume fraction of porosity (ϕ_2) is regarded as the sum of the measured values. The values of ϕ_2 and the corresponding trend lines are shown in Fig. 7(c). In this simulation, it is assumed that the ϕ_2 increases linearly with the W/C corresponding to the trend line, which can be expressed as $\phi_2 = 1.0048$ W/C + 2.6893 (Fig. 7(c)), where W/C denotes the water-to-cement ratio.

4.3. Parametric study and experimental comparisons

Numerical study is carried out to investigate the influence of the waviness of MWCNTs on the proposed micromechanics-based model, the results of which are illustrated in Fig. 8(a). Similar to previous studies [39,40], the bending of the MWCNT has a significant effect on the overall electrical behavior of the material. Fig. 8(b) shows that the effect of swarm size on the normalized root mean square error (NRMSE) and normalized computational cost (NCC). Herein, four different sizes of swarm are considered (10, 30, 50, and 100). The simulation accuracy is improved as the size of swarm increases, while the computational

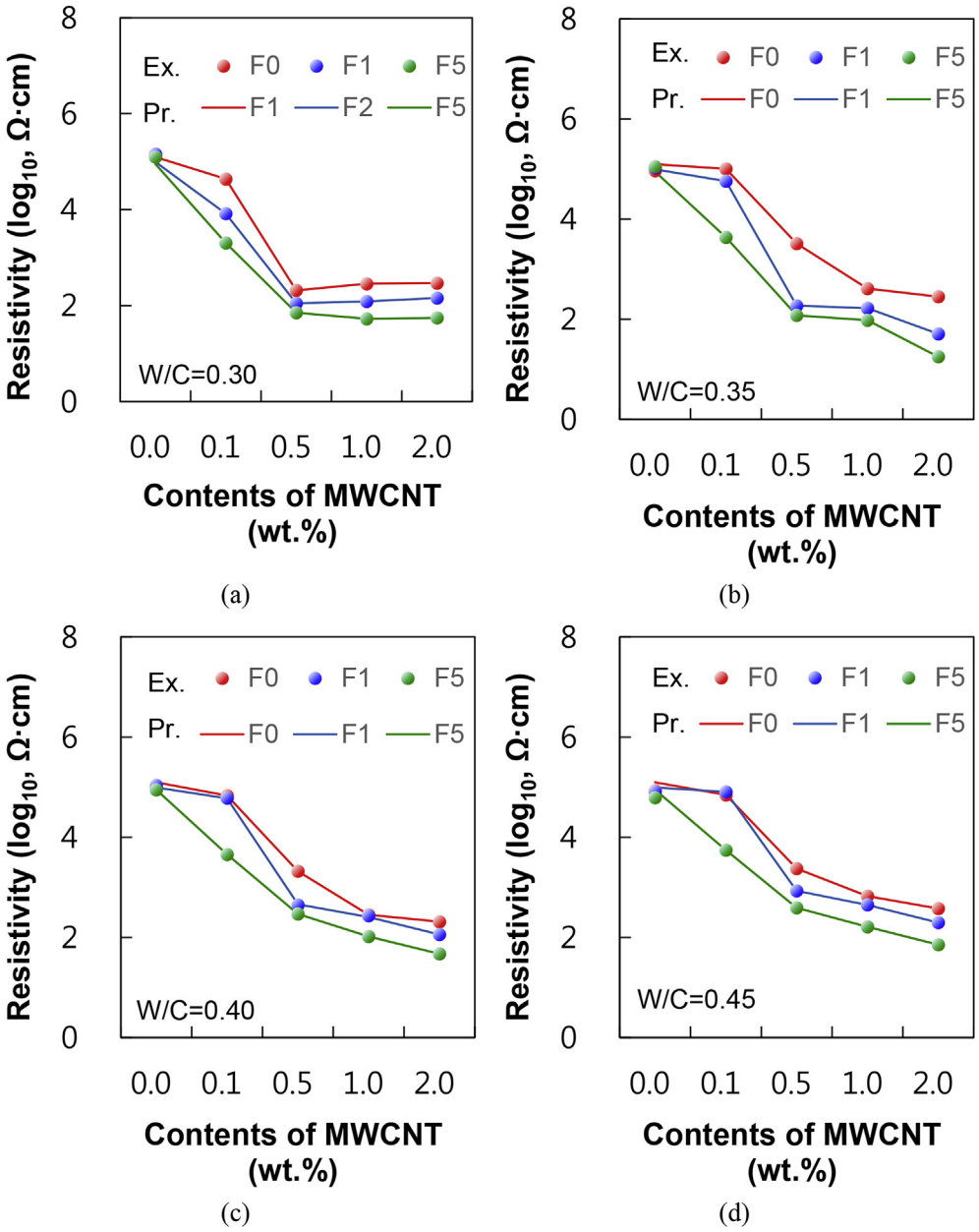

Fig. 9. Comparisons between experimental data and predictions based on the micromechanics with PSO algorithm.

cost exponentially increases. It shows that NRMSE is not much different when the swarm size is 50 and 100; however, the NCC rises more than double while swarm size increases from 50 to 100. Based on the simulation results, swarm size is fixed at 50 in this study, and all PSO calculations are performed under the same conditions. The micromechanics-based equation with the unknown model constant θ and the experimental results are computationally compared by the PSO algorithm, and the results are shown in Fig. 9. It can be seen in Fig. 9(a)-9(d) that the accuracy of simulation and experiment is very high for all cases.

Based on the PSO results, we proposed a simple formula for θ, which are the most critical factors for cementitious composites. This formula allows the processes of repeated unnecessary experimental-computational comparisons. Ultimately, a simpler method of determining the electrical properties and mixing ratio of the cement composite would be helpful. Fig. 10(a) summarizes the values of θ derived from the results of Fig. 9. It is found from Fig. 10(a) that, as ϕ_1 and W/C increase, the value of θ increases. The trends of θ with varying ϕ_1 and W/C are averaged after being traced, and are expressed as a single equation that can represent all cases ($\theta = 9\,\mathrm{W/C}\cdot e(50\cdot\phi_1) - \mathrm{W/C}\cdot\phi_1$). From the equation, we could roughly describe the tendency of θ with varying ϕ_1 and W/C. Fig. 10(c) shows the result of applying the equation illustrated in Fig. 10(b), which is simplified by tracing the pattern of θ to the developed micromechanical model. It is confirmed that the prediction of electrical performance is very rapid and relatively accurate when the averaged equation obtained by PSO algorithm is applied.

5. Conclusions

This study presents a modeling strategy that relies on various experimental results, micromechanics, and a PSO algorithm to estimate the electrical resistivity of MWCNT and CF-embedded cement composite. The proposed method enables reliable prediction of electrified cementitious complex materials, not only with respect to the electrical properties but also to the internal conductivity network conditions. In the future, more stable and developed computational algorithms could

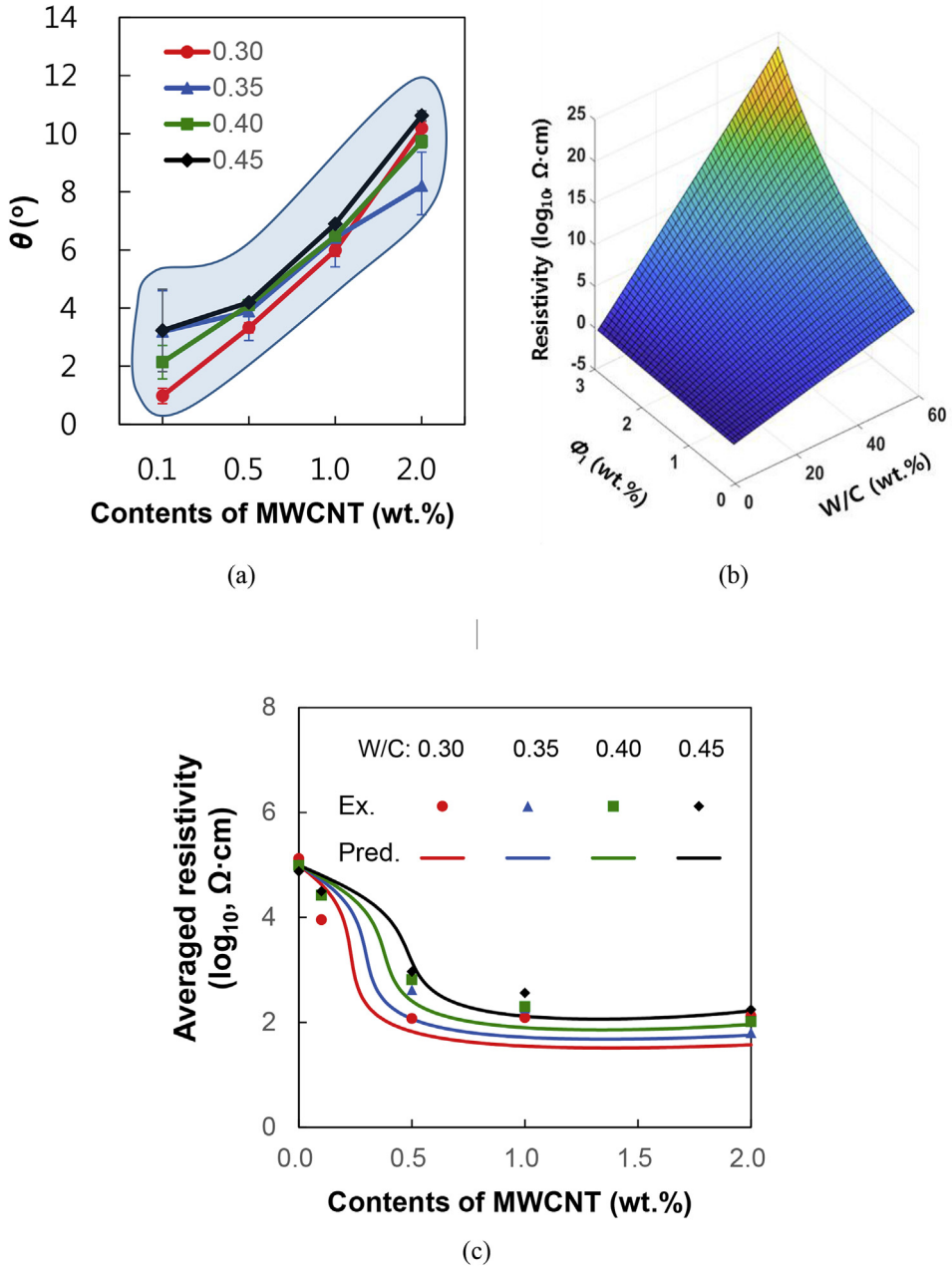

Fig. 10. (a) Trends in θ derived by combining experimental results with PSO algorithm, (b) predicted contour of θ according to W/C and ϕ_1, and (c) average of the experimental comparisons calculated by applying the new simplification method.

be coupled from the present study in order to analyze the various functionalities of advanced materials. The findings from the study are summarized below.

- A data-driven model based on 3-step hierarchical micromechanics and PSO is proposed to predict the electrical properties and mixing ratio of a conductive cement composite.
- The cement composite specimens with various MWCNT, CF, and W/C content are fabricated for use in the proposed model.
- Image processing technique, thermographic camera, 3D micro-CT, SEM image analysis, and two-probe method are utilized for data generation and quantitative evaluation of the specimens.
- The most influential model constant is considered to be the waviness of MWCNT, and a comparison between experiment and simulation based on the assumption shows very high prediction performance.
- Based on all the results, we proposed a formula for θ, in which a function of ϕ_1 and W/C. This formula enables improvement of the acceleration and accuracy of subsequent experimental and theoretical studies.

Acknowledgements

This study was supported by newly appointed professor research fund of Hanbat National University in 2017.

Appendix A. Supplementary data

Supplementary data to this article can be found online at https://doi.org/10.1016/j.compositesb.2018.12.011.

References

[1] Agrawal A, Choudhary A. Perspective: materials informatics and big data: realization of the “fourth paradigm” of science in materials science. Apl Mater 2016;4:053208.
[2] Han B, Sun S, Ding S, Zhang L, Yu X, Ou J. Review of nanocarbon-engineered multifunctional cementitious composites. Compos Appl Sci Manuf 2015;70:69–81.
[3] Singh AP, Gupta BK, Mishra M, Chandra A, Mathur R, Dhawan S. Multiwalled carbon nanotube/cement composites with exceptional electromagnetic interference shielding properties. Carbon 2013;56:86–96.
[4] Vitousek PM, Mooney HA, Lubchenco J, Melillo JM. Human domination of Earth's ecosystems. Science 1997;277:494–9.
[5] Li H, Zhang Q, Xiao H. Self-deicing road system with a CNFP high-efficiency thermal source and MWCNT/cement-based high-thermal conductive composites. Cold Reg Sci Technol 2013;86:22–35.
[6] Yehia S, Tuan CY, Ferdon D, Chen B. Conductive concrete overlay for bridge deck deicing: mixture proportioning, optimization, and properties. ACI Mater J 2000;97:172–81.
[7] Guan H, Liu S, Duan Y, Cheng J. Cement based electromagnetic shielding and absorbing building materials. Cement Concr Compos 2006;28:468–74.
[8] Wen S, Chung D. Seebeck effect in carbon fiber-reinforced cement. Cement Concr Res 1999;29:1989–93.
[9] Wen S, Chung D. Enhancing the Seebeck effect in carbon fiber-reinforced cement by using intercalated carbon fibers. Cement Concr Res 2000;30:1295–8.
[10] Argatov I, Sevostianov I. Health monitoring of bolted joints via electrical conductivity measurements. Int J Eng Sci 2010;48:874–87.
[11] Durgun E, Manzano H, Kumar P, Grossman JC. The characterization, stability, and reactivity of synthetic calcium silicate surfaces from first principles. J Phys Chem C 2014;118:15214–9.
[12] Shahsavari R, Buehler MJ, Pellenq RJM, Ulm FJ. First-principles study of elastic constants and interlayer interactions of complex hydrated oxides: case study of tobermorite and jennite. J Am Ceram Soc 2009;92:2323–30.
[13] Pellenq RJ-M, Kushima A, Shahsavari R, Van Vliet KJ, Buehler MJ, Yip S, Ulm F-J. A realistic molecular model of cement hydrates. Proc Natl Acad Sci Unit States Am 2009;106:16102–7.
[14] Qomi MA, Krakowiak K, Bauchy M, Stewart K, Shahsavari R, Jagannathan D, Brommer DB, Baronnet A, Buehler MJ, Yip S. Combinatorial molecular optimization of cement hydrates. Nat Commun 2014;5:4960.
[15] Wang M, Chung D. Understanding the increase of the electric permittivity of cement caused by latex addition. Compos B Eng 2018;134:177–85.
[16] Kim GM, Yang BJ, Yoon HN, Lee HK. Synergistic effects of carbon nanotube and carbon fiber on heat generation and electrical characteristics of cementitious composites. Carbon 2018;134:283–92.
[17] Nam I, Kim H, Lee H. Influence of silica fume additions on electromagnetic interference shielding effectiveness of multi-walled carbon nanotube/cement composites. Constr Build Mater 2012;30:480–7.
[18] Kim H, Nam I, Lee H. Enhanced effect of carbon nanotube on mechanical and electrical properties of cement composites by incorporation of silica fume. Compos Struct 2014;107:60–9.
[19] Kim G, Yang B, Cho K, Kim E, Lee H. Influences of CNT dispersion and pore characteristics on the electrical performance of cementitious composites. Compos Struct 2017;164:32–42.
[20] Pichler B, Hellmich C. Upscaling quasi-brittle strength of cement paste and mortar: a multi-scale engineering mechanics model. Cement Concr Res 2011;41:467–76.
[21] Pichler B, Hellmich C, Eberhardsteiner J, Wasserbauer J, Termkhajornkit P, Barbarulo R, Chanvillard G. Effect of gel–space ratio and microstructure on strength of hydrating cementitious materials: an engineering micromechanics approach. Cement Concr Res 2013;45:55–68.
[22] Königsberger M, Hlobil M, Delsaute B, Staquet S, Hellmich C, Pichler B. Hydrate failure in ITZ governs concrete strength: a micro-to-macro validated engineering mechanics model. Cement Concr Res 2018;103:77–94.
[23] Königsberger M, Irfan-ul-Hassan M, Pichler B, Hellmich C. Downscaling based identification of nonaging power-law creep of cement hydrates. J Eng Mech 2016;142:04016106.
[24] Irfan-ul-Hassan M, Königsberger M, Reihsner R, Hellmich C, Pichler B. How water-aggregate interactions affect concrete creep: multiscale Analysis. J Nanomech Micromech 2017;7:04017019.
[25] Damrongwiriyanupap N, Scheiner S, Pichler B, Hellmich C. Self-consistent channel approach for upscaling chloride diffusivity in cement pastes. Transport Porous Media 2017;118:495–518.
[26] García-Macías E, D'Alessandro A, Castro-Triguero R, Pérez-Mira D, Ubertini F. Micromechanics modeling of the electrical conductivity of carbon nanotube cement-matrix composites. Compos B Eng 2017;108:451–69.
[27] Hashemi R, Weng GJ. A theoretical treatment of graphene nanocomposites with percolation threshold, tunneling-assisted conductivity and microcapacitor effect in AC and DC electrical settings. Carbon 2016;96:474–90.
[28] Souri H, Yu J, Jeon H, Kim JW, Yang C-M, You N-H, Yang B. A theoretical study on the piezoresistive response of carbon nanotubes embedded in polymer nanocomposites in an elastic region. Carbon 2017;120:427–37.
[29] Wang Y, Weng GJ, Meguid SA, Hamouda AM. A continuum model with a percolation threshold and tunneling-assisted interfacial conductivity for carbon nanotube-based nanocomposites. J Appl Phys 2014;115:193706.
[30] Yang B, Jang J-u, Eem S-H, Kim SY. A probabilistic micromechanical modeling for electrical properties of nanocomposites with multi-walled carbon nanotube morphology. Compos Appl Sci Manuf 2017;92:108–17.
[31] Kim SY, Jang HG, Yang C-M, Yang B. Multiscale prediction of thermal conductivity for nanocomposites containing crumpled carbon nanofillers with interfacial characteristics. Compos Sci Technol 2018;155:169–76.
[32] Park M, Park JH, Yang BJ, Cho J, Kim SY, Jung I. Enhanced interfacial, electrical, and flexural properties of polyphenylene sulfide composites filled with carbon fibers modified by electrophoretic surface deposition of multi-walled carbon nanotubes. Compos Appl Sci Manuf 2018;109:124–30.
[33] Mayercsik NP, Felice R, Ley MT, Kurtis KE. A probabilistic technique for entrained air void analysis in hardened concrete. Cement Concr Res 2014;59:16–23.
[34] Kennedy J. Particle swarm optimization. Encyclopedia of machine learning. Springer; 2011. p. 760–6.
[35] Eberhart RC, Shi Y. Computational intelligence: concepts to implementations. Elsevier; 2011.
[36] Kennedy J, Eberhart R. Particle swarm optimization. IEEE international conference on neural networks. 1995. p. 1942–8.
[37] Lee S-M. Coevolutionary model predictive formation control and localization of swarm robotic systems, Doctoral thesis. Korea advanced institute of science and technology. 2014.
[38] Park HM, Kim G, Lee SY, Jeon H, Kim SY, Kim M, Kim JW, Jung YC, Yang B. Electrical resistivity reduction with pitch-based carbon fiber into multi-walled carbon nanotube (MWCNT)-embedded cement composites. Constr Build Mater 2018;165:484–93.
[39] Li C, Thostenson ET, Chou T-W. Effect of nanotube waviness on the electrical conductivity of carbon nanotube-based composites. Compos Sci Technol 2008;68:1445–52.
[40] Wang X, Bradford PD, Liu W, Zhao H, Inoue Y, Maria J-P, Li Q, Yuan F-G, Zhu Y. Mechanical and electrical property improvement in CNT/Nylon composites through drawing and stretching. Compos Sci Technol 2011;71:1677–83.